2-22-2018

Power-law scaling of extreme dynamics near higher-order exceptional points

Q. Zhong
Michigan Technological University

Demetrios N. Christodoulides
University of Central Florida

M. Khajavikhan
University of Central Florida

K. G. Makris
University of Crete

Ramy El-Ganainy
Michigan Technological University

Follow this and additional works at: https://digitalcommons.mtu.edu/physics-fp

 Part of the Dynamic Systems Commons, and the Physics Commons

Rapid Communications

Power-law scaling of extreme dynamics near higher-order exceptional points

Q. Zhong,[1] D. N. Christodoulides,[2] M. Khajavikhan,[2] K. G. Makris,[3] and R. El-Ganainy[1,4,*]
[1]*Department of Physics, Michigan Technological University, Houghton, Michigan 49931, USA*
[2]*College of Optics & Photonics-CREOL, University of Central Florida, Orlando, Florida 32816, USA*
[3]*Department of Physics, University of Crete, Heraklion 71003, Greece*
[4]*Henes Center for Quantum Phenomena, Michigan Technological University, Houghton, Michigan 49931, USA*

(Received 26 October 2017; published 22 February 2018)

We investigate the extreme dynamics of non-Hermitian systems near higher-order exceptional points in photonic networks constructed using the bosonic algebra method. We show that strong power oscillations for certain initial conditions can occur as a result of the peculiar eigenspace geometry and its dimensionality collapse near these singularities. By using complementary numerical and analytical approaches, we show that, in the parity-time ($\mathcal{PT}$) phase near exceptional points, the logarithm of the maximum optical power amplification scales linearly with the order of the exceptional point. We focus in our discussion on photonic systems, but we note that our results apply to other physical systems as well.

DOI: 10.1103/PhysRevA.97.020105

I. INTRODUCTION

One of the intriguing features of non-Hermitian Hamiltonians is the breakdown of eigenstate orthogonality (as defined by the Hermitian inner product) [1]. In the most extreme case, two or more distinct eigenstates can even become identical (share the same eigenvalue and eigenvector), giving rise to an eigenspace dimensionality collapse at the so-called exceptional points [2–7]. An exceptional point of order N (denoted as EPN) is formed by the coalescence of N eigenvectors to form an "exceptional vector." The incompleteness of the eigenbases at these special points leads to important consequences, such as the divergence of the Petermann factor [8–12] and ultrasensitivity to external perturbations [13,14]. While systems exhibiting EP2 have been intensively investigated both at the theoretical and experimental levels, higher-order EPs (mostly of order three) have so far received little attention [15–21], partly due to implementation difficulties in the laboratory. Recently, however, two groundbreaking experimental works have successfully demonstrated systems operating at a third-order exceptional point using acoustic [22] and optical [23] platforms. More complex schemes supporting even higher-order exceptional points can be constructed by using bosonic algebra [17].

Even though higher-order EPs are expected to demonstrate most of the general features of their counterpart second-order singularities, a quantitative description of the extreme dynamics near EPN is still lacking. In particular, power oscillations near EP2 in parity-time- ($\mathcal{PT}$-) symmetric systems have been investigated in Refs. [24–27]. Additionally, transient power growth in non-Hermitian optical setups has been recently studied using pseudospectrum techniques [28]. Here, we investigate the extreme dynamics in a $\mathcal{PT}$-symmetric [29–46] Hamiltonian having higher-order EPs [17].

By employing complementary numerical and analytical approaches, we are able to quantify the maximum value of the extreme optical power amplification for any higher-order EPN when the system approaches it from the $\mathcal{PT}$ phase. The main results of our work are as follows: (1) establishing the link between the dynamical evolution near EPs and the geometry of the eigenbases associated with the underlying $\mathcal{PT}$ system; and (2) demonstrating that the maximum power amplification follows a power-law dependency on the order N of the EP. Though our results are very general, for illustration purposes, we concentrate in our discussion on photonic implementations.

In the remainder of this Rapid Communication, for the sake of generality, we use dimensionless quantities. Physical parameters can be always calculated depending on the details of the physical system of interest.

II. POWER OSCILLATIONS NEAR EXCEPTIONAL POINTS: A GEOMETRIC PERSPECTIVE

Consider a discrete non-Hermitian Hamiltonian H of dimensions $N \times N$ (we do not treat infinite-dimension cases here). Within the optical coupled-mode formalism, this Hamiltonian can describe, for example, an array of coupled waveguides or resonators, and will obey the equation $i\frac{d\boldsymbol{a}}{dz} = H\boldsymbol{a}$. Here, $\boldsymbol{a} = (a_0, a_1, \ldots, a_{N-1})^T$ is the electric field amplitude vector and, assuming coupled waveguides, z is the propagation distance (for coupled cavities, z is replaced by the evolution time t). Suppose $\boldsymbol{e}_k$ are the right eigenvectors of H. Nonorthogonality implies that $\langle \boldsymbol{e}_k, \boldsymbol{e}_l \rangle = \boldsymbol{e}_k^* \cdot \boldsymbol{e}_l \neq 0$, where $\langle\ \rangle$ is the Hermitian inner product, the symbol "$*$" is the complex conjugate, and "$\cdot$" denotes the vector product without any further conjugation. A non-Hermitian inner product that restores orthogonality (also called biorthogonality) can be also defined, $\langle \tilde{\boldsymbol{e}}_k, \boldsymbol{e}_l \rangle = \boldsymbol{e}_k \cdot \boldsymbol{e}_l = 0$ $(k \neq l)$, where $\tilde{\boldsymbol{e}}_k = \boldsymbol{e}_k^*$ is the transpose of the left eigenvectors of H.

The general solution for the equation of motion for H is $\boldsymbol{a}(z) = \sum_{k=1}^{N} C_k \boldsymbol{e}_k \exp(-i\lambda_k z)$, where λ_k are eigenvalues

*Corresponding author: ganainy@mtu.edu

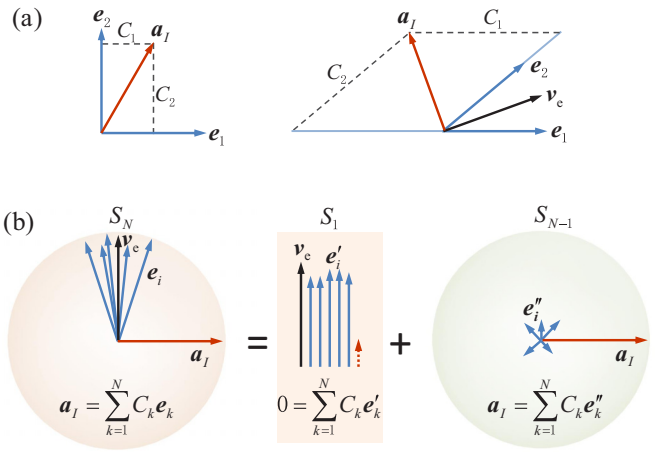

FIG. 1. Geometric intuitive illustrations of the origin of extreme fluctuations in the vicinity of exceptional points in two- and N-dimensional spaces as described in detail in the text are depicted in (a) and (b), respectively. In (b), the vectors $\boldsymbol{e}'_i$ and $\boldsymbol{e}''_i$ are components of $\boldsymbol{e}_i$ in the directions parallel and perpendicular to $\boldsymbol{v}_e$, respectively. Since the components $\boldsymbol{e}''_i$ are small and the vector $\boldsymbol{a}_I$ is orthogonal to $\boldsymbol{v}_e$, it follows that the coefficients C_k must have large values.

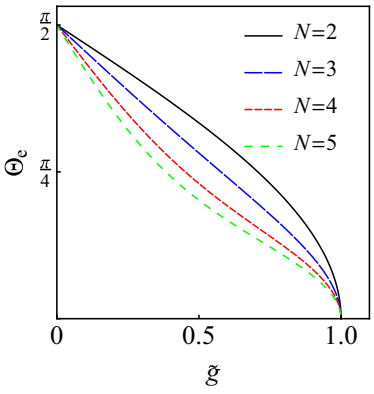

FIG. 2. The minimum Hermitian angle Θ_e between any two eigenvectors of the $\mathcal{PT}$ Hamiltonians H_N for different values of N as a function of the non-Hermitian parameter $\tilde{g}$. Clearly, Θ_e is smaller for larger N, indicating a faster eigenspace dimensionality collapse near higher-order exceptional points. This in turn suggests that more violent dynamics takes place near EPN with higher orders. Our analysis in the next section confirms and quantifies this prediction.

of H and the coefficients C_k are determined by the initial condition $\boldsymbol{a}_I = \boldsymbol{a}(z=0) = \sum_{k=1}^{N} C_k \boldsymbol{e}_k$. In the rest of this work, we will use the normalization $\langle \boldsymbol{e}_k, \boldsymbol{e}_k \rangle = \langle \boldsymbol{a}_I, \boldsymbol{a}_I \rangle = 1$. As a direct outcome of the non-Hermiticity, the total power $P(z) \equiv \langle \boldsymbol{a}(z), \boldsymbol{a}(z) \rangle$ is not conserved but rather varies along the propagation distance. In non-Hermitian systems that do not exhibit gain, the evolution of $P(z)$ will be decaying oscillations. We are interested mainly in the oscillatory part which, in some cases, can be isolated by a simple gauge transformation that results in a $\mathcal{PT}$-symmetric Hamiltonian [31]. The oscillatory behavior of these systems can be quantified either by using the total power behavior $P(z)$ or its z-averaged value $\langle P \rangle \equiv \frac{1}{L} \int_0^L P(z) dz$, where for perfect periodic variation L is the period of one cycle and otherwise $L \to \infty$. In this section we will use the latter to develop the geometric intuition behind the phenomenon of extreme power oscillation near EPs. An obvious advantage of using $\langle P \rangle$ is its direct dependence on the coefficients C_k, $\langle P \rangle = \sum_{k=1}^{N} |C_k|^2$. By considering the geometry of the nonorthogonal eigenbases, we now show that the quantity $\langle P \rangle$ takes large values in the vicinity of an exceptional point, which in turn indicates large oscillatory amplitudes.

Let us first focus on the simple case of a second-order exceptional point, EP2. As demonstrated in Fig. 1(a), in an orthogonal coordinate system (left panel) the projections of any vector cannot exceed the length of the vector itself. On the other hand, if the two basis vectors are almost parallel, a vector which is nearly orthogonal to the bases can exhibit very large projection coefficients, diverging in the limit when the two base vectors become identical, thus signaling the incompleteness of the bases. This argument can be generalized to higher dimensions, as demonstrated schematically in Fig. 1(b). Particularly, if an $N \times N$ Hamiltonian H exhibits an exceptional point of order N, EPN, all the eigenvectors of H become nearly "parallel" to the exceptional vector $\boldsymbol{v}_e$ (the notion of parallel vectors is defined here in the Hermitian sense). Thus the projection coefficients of a vector $\boldsymbol{a}_I$ which lies in an $N-1$ hyperplane orthogonal to $\boldsymbol{v}_e$ are large, implying a large value of $\langle P \rangle$. This behavior can be also understood by using the notion of biorthogonality. Particularly, since $C_k = \langle \tilde{\boldsymbol{e}}_k, \boldsymbol{a}_I \rangle / \langle \tilde{\boldsymbol{e}}_k, \boldsymbol{e}_k \rangle$ and by noting that the "complex length" of the exceptional vector (i.e., the quantity $\sqrt{\langle \boldsymbol{v}_e, \boldsymbol{v}_e \rangle}$) is zero, it is clear that C_k becomes larger when $\boldsymbol{e}_k \sim \boldsymbol{v}_e$ as long as $\langle \tilde{\boldsymbol{e}}_k, \boldsymbol{a}_I \rangle > \langle \tilde{\boldsymbol{e}}_k, \boldsymbol{e}_k \rangle$, which can happen when $\boldsymbol{a}_I \perp \boldsymbol{v}_e$ (though this is not necessarily guaranteed for all vectors in the orthogonal subspace).

Having presented this intuitive picture, we next proceed by considering a concrete example of $\mathcal{PT}$-symmetric Hamiltonians having higher-order exceptional points [17],

$$H_N = \begin{bmatrix} ig_0 & \kappa_0 & \cdots & 0 & 0 \\ & & \vdots & & \\ \cdots & \kappa_{n-1} & ig_n & \kappa_n & \cdots \\ & & \vdots & & \\ 0 & 0 & \cdots & \kappa_{N-2} & ig_{N-1} \end{bmatrix}, \qquad (1)$$

where the non-Hermitian (gain or loss) and coupling coefficients follow the rules $g_n = g(2n - N + 1)$ and $\kappa_n = \kappa\sqrt{(n+1)(N-n-1)}$ $(n = 0, 1, 2, \ldots, N-1)$, with the real-valued quantities g and κ representing scaling parameters. The reason for the unusual numbering of the matrix elements (starting from 0 instead of 1) will be clear in the next section. As has been shown in Ref. [17], H_N generalizes the canonical $\mathcal{PT}$-symmetric toy model H_2. Particularly, when $\tilde{g} \equiv g/\kappa < 1$, H_N is in the $\mathcal{PT}$ phase. The transition to the broken phase ($\tilde{g} > 1$) is marked by an Nth-order exceptional point at $\tilde{g} = 1$. Here, we are interested in the situation where g approaches κ from below where the system is still in the $\mathcal{PT}$ phase.

One possible measure to characterize the relationship between the eigenvectors of H_N is the Hermitian angle [47,48], which is defined between two complex vectors $\boldsymbol{v}$ and $\boldsymbol{u}$ as $\cos\Theta(\boldsymbol{v}, \boldsymbol{u}) \equiv \frac{|\langle \boldsymbol{v}, \boldsymbol{u} \rangle|}{|\boldsymbol{v}||\boldsymbol{u}|}$ with $\Theta(\boldsymbol{v}, \boldsymbol{u}) \in [0, \pi/2]$. Figure 2 presents a comparison between the minimum Hermitian angle Θ_e

associated with the eigenvectors of H_N for different values of N. Note that Θ_e is smaller for larger values of N, indicating a faster collapse of the eigenspace dimensionality as $\tilde{g} \to 1$. Consequently, one expects more "violent" power oscillation for larger N values. In the following section, we confirm and quantify this behavior analytically.

III. EXACT RESULTS USING BOSONIC ALGEBRA

In this section, we employ the bosonic algebra method to study spectrum and propagation dynamics of a system described by H_N. In contrast to the previous section, here we focus on $P(z)$ rather than its z average.

To do so, we consider the non-Hermitian two-side noninteracting Bose-Hubbard model that was used to construct H_N,

$$\hat{H} = -ig(\hat{b}_1^\dagger \hat{b}_1 - \hat{b}_2^\dagger \hat{b}_2) + \kappa(\hat{b}_1^\dagger \hat{b}_2 + \hat{b}_1 \hat{b}_2^\dagger), \tag{2}$$

where $\hat{b}_{1,2}^\dagger$ and $\hat{b}_{1,2}$ are the bosonic creation and annihilation operators of oscillators 1 and 2, and we assumed $\hbar = 1$. In the bases $|N_p - n, n\rangle$ representing a Fock state with $N_p - n$ and n bosons in sites 1 and 2, respectively (i.e., a total number of N_p bosonic particles), the matrix representation of $\hat{H}$ is H_N [17], where $N = N_p + 1$.

Before we proceed, we emphasize that the model in Eq. (2) does not represent an actual $\mathcal{PT}$-symmetric quantum system [37,49–51] but is rather used as a mathematical tool to facilitate the analysis. Motivated by the fact that the Hamiltonian H_N is generated from $\hat{H}$ in Eq. (2) by populating the latter with N_p particles and by noting that $\hat{H}$ is obtained from quantizing H_2 [17], we now focus on the $\hat{H}$ and consider the following normalized input state at $z = 0$, $|I(q_1,q_2)\rangle = \frac{1}{\sqrt{N_p!}}(q_1\hat{b}_1^\dagger + q_2\hat{b}_2^\dagger)^{N_p}|0,0\rangle$ with $|q_1|^2 + |q_2|^2 = 1$. This state can be also cast in the form $|I(q_1,q_2)\rangle = \sum_{n=0}^{N_p} a_n |N_p - n, n\rangle$ with the expansion coefficients given by $a_n = \sqrt{\frac{N_p!}{(N_p-n)!n!}} q_1^{N_p-n} q_2^n$. Although this particular construction of $|I(q_1,q_2)\rangle$ does not span all the vector space when $N_p > 1$, we will see later that it suffices for our calculations.

The output state at distance z can be written as (see Appendix A for the derivation)

$$\begin{aligned} |O\rangle &= e^{-i\hat{H}z}|I\rangle \\ &= \frac{1}{\sqrt{N_p!}}[q_1(z)\hat{b}_1^\dagger + q_2(z)\hat{b}_2^\dagger]^{N_p}|0,0\rangle \\ &= \sum_{n=0}^{N_p} a_n(z)|N_p - n, n\rangle, \end{aligned} \tag{3}$$

where $a_n(z) = \sqrt{\frac{N_p!}{(N_p-n)!n!}}[q_1(z)]^{N_p-n}[q_2(z)]^n$ with the z-dependent quantities $q_1(z) = q_1U_{11}(z) + q_2U_{21}(z)$ and $q_2(z) = q_1U_{12}(z) + q_2U_{22}(z)$ and the elements of $U(z) \equiv e^{-iH_2z}$ are

$$U(z) = \begin{bmatrix} \cos(\lambda z) - \frac{g}{\lambda}\sin(\lambda z) & -i\frac{\kappa}{\lambda}\sin(\lambda z) \\ -i\frac{\kappa}{\lambda}\sin(\lambda z) & \cos(\lambda z) + \frac{g}{\lambda}\sin(\lambda z) \end{bmatrix}, \tag{4}$$

where $\lambda = \sqrt{\kappa^2 - g^2}$.

Note that within the coupled-mode formalism of waveguide (or cavity) arrays, the states $|N_p - n, n\rangle$ represent the waveguide number n while the coefficients $a_n(z)$ describe the associated field amplitudes (see Ref. [17] for more details). Therefore, the total power is given by $P(z) = \sum_{n=0}^{N-1} |a_n(z)|^2$. When the input power is taken to be unity, the expression for the maximum amplification thus becomes $G_N = \max[P_N(z)]$.

For the case of $N = 2$, it is easy to show that, apart from a phase factor, the initial optimal vector leading to the maximum amplification is $\boldsymbol{a}_I^{\text{opt}} = (q_1,q_2)^T = \frac{1}{\sqrt{2}}(1, -i)^T$. Under these conditions, the power oscillation dynamics is given by

$$P_2^{\text{opt}}(z) = 1 + \frac{2\tilde{g}}{1-\tilde{g}}\sin^2(\lambda z), \tag{5}$$

and this initial condition lets $G_2 = \frac{1+\tilde{g}}{1-\tilde{g}}$. Note that the Hermitian angle between $\boldsymbol{a}_I^{\text{opt}}$ and $\boldsymbol{v}_e$ is $\pi/2$, i.e., $\boldsymbol{a}_I^{\text{opt}}$ is orthogonal to $\boldsymbol{v}_e$, in agreement with the discussion in the previous section.

The general case for $N > 2$ is more subtle. In principle, one has to choose the optimal initial vector that results in the maximum amplification from the set of all initial conditions $|I'\rangle = \sum_{n=0}^{N_p} q_n(\hat{b}_1^\dagger)^{N_p-n}(\hat{b}_2^\dagger)^n|0,0\rangle$. The input state $|I\rangle$, however, describes only a subset of all initial states. Within this subspace, it is straightforward to show that even when $N > 2$, the optimal vector still corresponds to $|I(q_1,q_2)\rangle$ with $(q_1,q_2) = \frac{1}{\sqrt{2}}(1, -i)$. In that case, the power dynamics and the maximum G_N are given by (see Appendix B)

$$P_N^{\text{opt}}(z) = \left[1 + \frac{2\tilde{g}}{1-\tilde{g}}\sin^2(\lambda z)\right]^{N-1}, \tag{6}$$

and

$$G_N(\tilde{g}) = \max\left[P_N^{\text{opt}}(z)\right] = \left(\frac{1+\tilde{g}}{1-\tilde{g}}\right)^{N-1}. \tag{7}$$

Note that here also $\boldsymbol{a}_I^{\text{opt}}$ is perpendicular to the exceptional vector $\boldsymbol{v}_e$ which in higher dimensions can be generated from the expression for $|I(q_1,q_2)\rangle$ by substituting $(q_1,q_2) = \frac{1}{\sqrt{2}}(1,i)$.

Even though Eq. (7) is derived by using a subset of all the possible initial conditions, we expect it to hold when all the possible initial conditions are considered since all the Hamiltonians H_N are generated from $\hat{H}$. To confirm this intuition, we will now employ a numerical technique based on singular value decomposition (SVD) to establish that the value of G_N as obtained by Eq. (7) indeed provides the global maximum [28]. This method is an exact optimization problem that determines the maximum possible optimal amplification for any given propagation distance z by considering all possible initial conditions. Furthermore, it determines the corresponding initial conditions that lead to such maximum power growth. In particular, it can be shown analytically that the maximum possible power amplification at a given z is equal to the largest singular value of the propagator of the problem or equivalently of the matrix norm of the propagator e^{-iH_Nz} (where the norm of a matrix M is generally defined $\|M\| \equiv \sup_{\boldsymbol{u}} \|M\boldsymbol{u}\|/\|\boldsymbol{u}\|$, where $\|\boldsymbol{u}\|$ is the usual Euclidean norm of the vector $\boldsymbol{u}$). In other words, we have $G_N^{\text{opt}}(z) = ||e^{-iH_Nz}||^2 = (\max[\sigma_N])^2$, where σ_N are the singular values associated with e^{-iH_Nz}. The right singular eigenvector of the propagator determines the specific initial conditions that lead to the maximum amplification. The

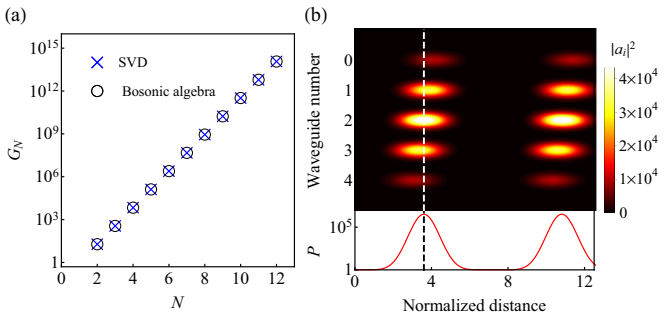

FIG. 3. (a) A plot of G_N and G'_N against N when ($\tilde{g} = 0.9$) given by Eq. (7) on a log scale. Clearly, the expression (7) for G_N provides the global value of the maximum amplification and it follows a power-law dependency on N. (b) Propagation dynamics in a waveguide array implementing a fifth-order EP, i.e., described by H_5, under the optimal input excitation, $\boldsymbol{a}_I = \frac{1}{4}(1, -2i, -\sqrt{6}, 2i, 1)^T$. The top panel presents the intensities in the individual waveguides while the lower panel plots the total intensity in normalized units. Note that the dynamics is oscillatory and that the maximum of the intensity in each waveguide does not necessarily occur at the same distance where the total intensity assumes its maximum value.

global maximum can be then found by maximizing $G_N^{\text{opt}}(z)$ with respect to z by scanning $z \in [0, L]$, to obtain $G'_N(\tilde{g}) = \max[G_N^{\text{opt}}(z)]$. Figure 3(a) depicts the values of G'_N and G_N versus the order of the exceptional point N on a log scale. A prefect agreement is found between the value of G_N and the global maximum as obtained by SVD.

Equation (7) is the central result of this Rapid Communication and demonstrates that maximum amplification is given by G_N and follows a power-law dependency on the order of the exceptional point, with oscillation dynamics becoming more pronounced for larger N. An interesting observation is that, when $\tilde{g} \sim 1$, one can recast G_N in the form $G_N(K_2) = (4K_2)^{N-1}$, where $K_2 = (1 - \tilde{g}^2)^{-1}$ is the Petermann factor associated with H_2.

Finally, we also study the propagation dynamics of the optimal initial condition for the case of H_5. Figure 3(b) presents the evolution of the power in the individual waveguides (top panel) as well as the total power (lower panel). An important observation here is that the propagation distance at which the total power attains its maximum value does not necessarily correspond to the maximum power in the individual channels.

IV. CONCLUDING REMARKS

In this Rapid Communication, we have investigated the behavior of $\mathcal{PT}$-symmetric systems having higher-order exceptional points. Our analysis, relying on the bosonic algebra method, showed that for systems operating near exceptional points, the maximum possible amplification scales with the power of N (the order of the EP). These results have been confirmed by employing an exact numerical optimization technique based on singular value decomposition. Given the recent success in implementing third-order exceptional points in acoustic and photonic systems and the continuing effort to realize even more complex structures, our results provide valuable insight into the generic behavior near EPs which may help direct future research in this field.

In addition, our work opens up a new set of intriguing questions that merit future investigations. For example, do systems having higher-order EPs exhibit the same dynamics locally close to the EPs? In such a case, the power-law dependency discovered here would be universal. However, it is also possible that Hamiltonians that do not have the form of H_N behave differently. We note, however, that, to date, Hamiltonians of the form H_N are the only systematic approach to realize arbitrarily higher-order EPs in discrete arrangements. Another interesting question is how nonlinear interactions come into play when the amplification leads to large intensities that trigger various nonlinear effects. One of the very important directions with practical consequences is the problem of the laser linewidth near EPs. Whereas a direct extrapolation from the original work of Petermann [8] predicts a divergent linewidth at EPs, a recent analysis by Yoo *et al.* [37] demonstrated that the linewidth enhancement is finite. Our work here provides an intuitive framework for understanding the amplification of noise near EPs and hints that even larger enhancement factors should be expected near higher-order EPs. It would be of interest to fully develop this link either by using an analysis similar to that of Ref. [37] or other statistical methods [52].

ACKNOWLEDGMENTS

The authors acknowledge support from the Army Research Office (ARO) Grant No. W911NF-17-1-0481. Q.Z. acknowledges support from China Scholarship Council (CSC).

APPENDIX A

Here, we present the derivation Eq. (3) in the main text. First, we note that $|O\rangle$ can be written as

$$\begin{aligned} |O\rangle &= e^{-i\hat{H}z}|I\rangle \\ &= \frac{1}{\sqrt{N_p!}} e^{-i\hat{H}z}(q_1\hat{b}_1^\dagger + q_2\hat{b}_2^\dagger)^{N_p} e^{i\hat{H}z} e^{-i\hat{H}z}|0,0\rangle \\ &= \frac{1}{\sqrt{N_p!}} [e^{-i\hat{H}z}(q_1\hat{b}_1^\dagger + q_2\hat{b}_2^\dagger)e^{i\hat{H}z}]^{N_p}|0,0\rangle , \end{aligned} \tag{A1}$$

where we used the fact that $e^{-i\hat{H}z}|0,0\rangle = |0,0\rangle$. Next, we define $\hat{b}_{1,2}^\dagger(z) \equiv e^{-i\hat{H}z}\hat{b}_{1,2}^\dagger e^{i\hat{H}z}$, which leads to the equation of motion $i\frac{d}{dz}(\hat{b}_1^\dagger(z), \hat{b}_2^\dagger(z))^T = H_2(\hat{b}_1^\dagger(z), \hat{b}_2^\dagger(z))^T$, admitting the formal solution $(\hat{b}_1^\dagger(z), \hat{b}_2^\dagger(z))^T = e^{-iH_2 z}(\hat{b}_1^\dagger, \hat{b}_2^\dagger)^T \equiv U(z)(\hat{b}_1^\dagger, \hat{b}_2^\dagger)^T$. By substituting in (A1), we then obtain

$$\begin{aligned} |O\rangle &= \frac{1}{\sqrt{N_p!}} [q_1\hat{b}_1^\dagger(z) + q_2\hat{b}_2^\dagger(z)]^{N_p}|0,0\rangle \\ &= \frac{1}{\sqrt{N_p!}} [q_1(z)\hat{b}_1^\dagger + q_2(z)\hat{b}_2^\dagger]^{N_p}|0,0\rangle , \end{aligned} \tag{A2}$$

where $q_{1,2}(z)$ are defined in the text. This completes the derivation.

APPENDIX B

Here, we present the derivation of expression (6) in the main text for a general N,

$$P_N(z) = \sum_{n=0}^{N_p} |a_n(z)|^2$$

$$= \sum_{n=0}^{N_p} \frac{N_p!}{(N_p-n)!n!} [|q_1(z)|^2]^{N_p-n} [|q_2(z)|^2]^n$$

$$= (|q_1(z)|^2 + |q_2(z)|^2)^{N_p}$$

$$= [P_2(z)]^{N-1}. \tag{B1}$$

[1] J. J. Sakurai and J. J. Napolitano, *Modern Quantum Mechanics*, 2nd ed. (Pearson, London, 2010).
[2] W. D. Heiss and A. L. Sannino, J. Phys. A **23**, 1167 (1990).
[3] A. I. Magunov, I. Rotter, and S. I. Strakhova, J. Phys. B **32**, 1669 (1999).
[4] W. D. Heiss, J. Phys. A **37**, 2455 (2004).
[5] W. D. Heiss, J. Phys. A **45**, 444016 (2012).
[6] I. Rotter, Phys. Rev. E **67**, 026204 (2003).
[7] M. Müller and I. Rotter, J. Phys. A **41**, 244018 (2008).
[8] K. Petermann, IEEE J. Quantum Electron. **15**, 566 (1979).
[9] A. E. Siegman, Phys. Rev. A **39**, 1253 (1989).
[10] G. H. C. New, J. Mod. Opt. **42**, 799 (1995).
[11] M. V. Berry, J. Mod. Opt. **50**, 63 (2003).
[12] S.-Y. Lee, J.-W. Ryu, J.-B. Shim, S.-B. Lee, S. W. Kim, and K. An, Phys. Rev. A **78**, 015805 (2008).
[13] J. Wiersig, Phys. Rev. Lett. **112**, 203901 (2014).
[14] J. Wiersig, Phys. Rev. A **93**, 033809 (2016).
[15] E. M. Graefe, U. Günther, H. J. Korsch, and A. E. Niederle, J. Phys. A **41**, 255206 (2008).
[16] D. Gilles and G. Eva-Maria, J. Phys. A **45**, 025303 (2012).
[17] M. H. Teimourpour, R. El-Ganainy, A. Eisfeld, A. Szameit, and D. N. Christodoulides, Phys. Rev. A **90**, 053817 (2014).
[18] W. D. Heiss and G. Wunner, J. Phys. A **48**, 345203 (2015).
[19] Z. Lin, A. Pick, M. Lončar, and A. W. Rodriguez, Phys. Rev. Lett. **117**, 107402 (2016).
[20] W. D. Heiss and G. Wunner, J. Phys. A **49**, 495303 (2016).
[21] H. Jing, S. K. Özdemir, H. Lü, and F. Nori, Sci. Rep. **7**, 3386 (2017).
[22] K. Ding, G. Ma, M. Xiao, Z. Q. Zhang, and C. T. Chan, Phys. Rev. X **6**, 021007 (2016).
[23] H. Hodaei, A. U. Hassan, S. Wittek, H. Garcia-Gracia, R. El-Ganainy, D. N. Christodoulides, and M. Khajavikhan, Nature (London) **548**, 187 (2017).
[24] R. El-Ganainy, K. G. Makris, D. N. Christodoulides, and Z. H. Musslimani, Opt. Lett. **32**, 2632 (2007).
[25] K. G. Makris, R. El-Ganainy, D. N. Christodoulides, and Z. H. Musslimani, Phys. Rev. Lett. **100**, 103904 (2008).
[26] Z. H. Musslimani, K. G. Makris, R. El-Ganainy, and D. N. Christodoulides, Phys. Rev. Lett. **100**, 030402 (2008).
[27] W. D. Heiss, Eur. Phys. J. D **60**, 257 (2010).
[28] K. G. Makris, L. Ge, and H. E. Türeci, Phys. Rev. X **4**, 041044 (2014).
[29] C. M. Bender and S. Boettcher, Phys. Rev. Lett. **80**, 5243 (1998).
[30] C. M. Bender, S. Boettcher, and P. N. Meisinger, J. Math. Phys. **40**, 2201 (1999).
[31] A. Guo, G. J. Salamo, D. Duchesne, R. Morandotti, M. Volatier-Ravat, V. Aimez, G. A. Siviloglou, and D. N. Christodoulides, Phys. Rev. Lett. **103**, 093902 (2009).
[32] C. E. Ruter, K. G. Makris, R. El-Ganainy, D. N. Christodoulides, M. Segev, and D. Kip, Nat. Phys. **6**, 192 (2010).
[33] Y. D. Chong, L. Ge, H. Cao, and A. D. Stone, Phys. Rev. Lett. **105**, 053901 (2010).
[34] S. Longhi, Phys. Rev. A **82**, 031801 (2010).
[35] Z. Lin, H. Ramezani, T. Eichelkraut, T. Kottos, H. Cao, and D. N. Christodoulides, Phys. Rev. Lett. **106**, 213901 (2011).
[36] J. Schindler, A. Li, M. C. Zheng, F. M. Ellis, and T. Kottos, Phys. Rev. A **84**, 040101(R) (2011).
[37] G. Yoo, H.-S. Sim, and H. Schomerus, Phys. Rev. A **84**, 063833 (2011).
[38] A. Regensburger, C. Bersch, M.-A. Miri, G. Onishchukov, D. N. Christodoulides, and U. Peschel, Nature (London) **488**, 167 (2012).
[39] L. Feng, Z. J. Wong, R.-M. Ma, Y. Wang, and X. Zhang, Science **346**, 972 (2014).
[40] H. Hodaei, M.-A. Miri, M. Heinrich, D. N. Christodoulides, and M. Khajavikhan, Science **346**, 975 (2014).
[41] B. Peng, S. K. Özdemir, F. Lei, F. Monifi, M. Gianfreda, G. L. Long, S. Fan, F. Nori, C. M. Bender, and L. Yang, Nat. Phys. **10**, 394 (2014).
[42] L. Chang, X. Jiang, S. Hua, C. Yang, J. Wen, L. Jiang, G. Li, G. Wang, and M. Xiao, Nat. Photonics **8**, 524 (2014).
[43] H. Jing, S. K. Özdemir, X.-Y. Lü, J. Zhang, L. Yang, and F. Nori, Phys. Rev. Lett. **113**, 053604 (2014).
[44] K. Makris, Z. Musslimani, D. N. Christodoulides, and S. Rotter, Nat. Commun. **6**, 7257 (2015).
[45] L. Ge, K. G. Makris, D. N. Christodoulides, and L. Feng, Phys. Rev. A **92**, 062135 (2015).
[46] O. I. Z. Gutiérrez, L. F. S. Mendoza, and B. M. Rodríguez-Lara, Opt. Express **24**, 3989 (2016).
[47] K. Scharnhorst, Acta Appl. Math. **69**, 95 (2001).
[48] A. Galantai and C. J. Hegedus, Numer. Linear Algebra Appl. **13**, 589 (2006).
[49] L. Jin and Z. Song, Phys. Rev. A **80**, 052107 (2009).
[50] X. Z. Zhang, L. Jin, and Z. Song, Phys. Rev. A **87**, 042118 (2013).
[51] S. Longhi, Phys. Rev. A **88**, 052102 (2013).
[52] M. O. Scully and M. S. Zubairy, *Quantum Optics*, 1st ed. (Cambridge University Press, Cambridge, U.K., 1997).